ISSN 2548-6462 (online), ISSN 2088-8740 (print)

DOI: 10.30644/rik.v12i1.761

Formulation of Fenofibrate Nanocrystals with Wet Milling Method

M. Henityo Agung As;adi[1*], Ilham Kuncahyo[2], Teuku Nanda Saifullah Sulaiman[3]
[1] Program Studi S2 Farmasi, Fakultas Farmasi, Universitas Setia Budi, Surakarta, Indonesia
[3] Program Studi Farmasi, Fakultas Farmasi, Universitas Gadjah Mada, Yogyakarta, Indonesia
*Email korespondensi : (agungasadi28@gmail.com)

Accepted: 3 June 2023; revision: 15 June 2023; published: 30 June 2023

Abstract

Background*: Fenofibrate is an antihyperlipidemic belonging to BCS class II, practically insoluble in water and has high lipophilicity, so it is proven that the inhibitor of the rate of absorption of fenofibrate from the digestive tract is slow to dissolve. This study aims to increase the solubility of fenofibrate by forming nanocrystals.*
Method*: Formation of nanocrystals using the wet milling method*
Result: *The fenofibrate nanocrystals produced a particle size of 775.966 nm, a zeta potential of -21.302 mV, and a solubility of 5.977 µg/mL.*
Conclusion *: The optimum formula with tween 80 components, grinding speed and grinding time in the manufacture of fenofibrate nanocrystals using the Factorial Design method obtained 0.2% tween 80, grinding speed of 500 rpm and grinding time of 1 hour. The critical parameter test results for the optimum formula obtained a particle size of 775.966 nm, a zeta potential of -21.302 mV and a solubility of 5.977 µg/mL. The DSC test showed that there was a difference in the melting point peaks and a decrease in crystal intensity between pure fenofibrate and fenofibrate nanocrystals. The FTIR test showed no difference in functional groups between pure fenofibrate and fenofibrate nanocrystals. The XRD test showed that there was a difference in peak crystal intensity between pure fenofibrate and fenofibrate nanocrystals. The SEM analysis shows that there are differences in shape and magnification used between pure fenofibrate and fenofibrate nanocrystals.*

Keyword: *nanocrystals, fenofibrate, particle size, solubility*

INTRODUCTION

Drug compounds that have low solubility in water (drugs that are poorly soluble) are a challenge in the development of new drugs. Solubility is one of the physicochemical properties of drug compounds that is important to note when formulating a drug substance into a dosage form (Khadka, 2014). There are several pharmaceutical strategies to increase the solubility and dissolution rate of drug substances in water, including: modifying the physical properties of drug substances, adding solubility enhancing agents, micronization, preparing solid dispersions, forming prodrugs, drug inclusion complexes with carriers, and modifying drug compounds. into salt and solvate (Retnowati & Setyawan, 2010).

Nanocrystals are crystals with sizes in the nanometer range, which means they are nanoparticles with a crystalline form. In the pharmaceutical world, the stated size of nanoparticles is in the range of 1-1000 nm (Junghanns, 2008). The manufacture of nanoparticles can be classified into two, namely the top-down method and the bottom-up method. The top-down method aims to reduce the particle size to the nanometer size range. Unlike the top-down method, the bottom-up method is prepared by dissolving the drug in a solvent, and undergoing precipitation, evaporation and crystallization processes (Chan et al., 2011).

Fenofibrate is an antihyperlipidemic belonging to BCS class II, practically insoluble in water (0.3µg / 37 mL) and has high lipophilicity (logP 5.3), so it is proven that inhibiting the rate of absorption of fenofibrate from the digestive tract is dissolution (Madgulkar , et al, 2019). According to (Ige et al., 2013) by decreasing the particle size from 80,000 ± 923 nm to 460 ± 20 nm, it can

significantly increase dissolution and bioavailability. Tests by test animals on New Zealand white rats showed an increase in bioavailability compared to pure drug. These BCS class II drugs have low bioavailability, with their absorption being limited by the dissolution rate (Chowdary & Enturi, 2011).

Poloxamer 188 is an FDA-approved difunctional block copolymer surfactant under the trade name Pluronic F68 (Yan et al., 2010). Poloxamer 188, also known as Pluronic F68, is a three-block copolymer of polyethylene oxide-polypropylene oxide-polyethylene oxide (PEO-PPO-PEO) used as a surfactant (Perecin et al., 2016). Poloxamer is a non-ionic linear triblock copolymer consisting of a central hydrophobic PPO segment and two hydrophilic PEO side segments. While hydrophilic PEO composes drug crystals providing a steric barrier and preventing particle aggregation and growth, adsorption on the crystal surface is driven by the hydrophobic interactions of the hydrophobic PPO chains (Tuomela et al., 2016).

Tween 80 is an ester of polyethylene sorbitol, with an calculated molecular weight of 1310 Da, with 20 units of ethylene oxide, one sorbitol, and one oleic acid as primary fatty acids. Tween 80 is widely used in biochemical applications, including dissolving proteins, isolating nuclei from cells in cell cultures, growing tubercle bacilli, and emulsifying and dispersing substances in medicinal and food products (Ma et al., 2011). Tween 80 has been widely used as a surfactant for nanocrystalline preparations, such as those of: (Rao et al., 2008), (B. Van Eerdenbrugh et al., 2007) and (X. Hu et al., 2017).

Important parameters of nanomilling to obtain optimal product: amount of drug and pearl milling size, milling speed, milling time and temperature. The milling time and speed required to obtain nanocrystals of the desired size range varies greatly. Nanocrystals are obtained either with low milling speed (80–90 rpm) and long milling time (1-5 days) or high milling speed (1800–4800 rpm) and short milling time (30-60 minutes) (Peltonen & Hirvonen , 2010). The effect of grinding speed and time has been carried out by (Choi et al., 2005).

Formulating fenofibrate with poloxamer 188 and tween 80 polymers using the high pressure homogenization method showed the formation of nano-sized particles (Madgulkar, et al, 2019). The wet milling method is one of the top-down methods where this method is capable of making nano-sized particulates as was done by (Bastami et al., 2015), (Ochi et al., 2014), (Karagianni & Peltonen, 2020). Previous research on fenofibrate was made of fenofibrate encapsulated nanocrystals using polyvinylpyrrolidone (PVP), polyvinyl alcohol (PVA) (Kumar & Siril, 2018), and fenofibrate film strips (Kevadiya et al., 2018), but there has been no research using this method. wet milling with fenofibrate using poloxamer 188 polymer and tween 80 surfactant.

METHOD

The design of this fenofibrate nanocrystal formulation uses the factorial design 2^3 method.

Table 1. Design Factor 2^3

Level	Formula		
	Tween 80 (%)	**Grinding Speed (rpm)**	**Grinding Time (hours)**
Low Level (-)	0,2	300	1
High Level (+)	0,6	500	2

Table 2. Rancangan Formulasi Nanokristal Fenofibrat Design Factor 2^3

Formula	Tween 80 (%)	Grinding Speed (rpm)	Grinding Time (Hours)
1	0,6	300	2
2	0,2	500	2
3	0,6	500	2
4	0,2	300	1
5	0,2	500	2
6	0,2	300	2
7	0,6	300	2
8	0,2	500	1
9	0,6	300	1
10	0,6	500	1
11	0,6	500	1
12	0,2	300	1

13	0,6	500	2
14	0,6	300	1
15	0,2	300	2
16	0,2	500	1

Nanosuspensions were prepared using a planetary ball mill (Retsch PM 100, Germany). Poloxamer 188 (0.2%) and Tween 80 were prepared in various ratios (Table 3) dissolved in water (polymer solution). Pure fenofibrate is mixed with a polymer solution, put into the chamber of the planetary ball mill. The planetary ball mill tool is run at various speeds and times (Table 3). Grinding was stopped every 5 minutes and then ground again for 5 minutes to prevent overheating, and a nanosuspension was formed. After grinding is complete, the nanosuspension is transferred to a clean container. The chamber is cleaned with sufficient aqua destillata, and the rinse water is placed in the nanosuspension container. The nanosuspension formed was then dried using the freeze drying method, mannitol was added to the nanosuspension as a cryoprotectant and a fenofibrate nanocrystal powder was formed which would then be evaluated (Colombo et al., 2017).

Particle Size Analyzer (PSA), Particle size analysis of the Fenofibrate made was carried out using Horiba SZ-100, the samples analyzed were samples that formed nanosuspensions (Colombo et al., 2017). The formed nanosuspension was put into the chamber with a little distilled water added, which was then analyzed for particle size. The average diameter and dispersion index of each group were recorded.

Zeta Potential, Zeta potential measurements were carried out using a Horiba SZ-100. The nanosuspension sample was diluted with distilled water and put into the tool and then analyzed for zeta potential (Colombo et al., 2017).

Solubility, The solubility test was carried out on microcrystalline and nanocrystalline fenofibrate. Weigh 10.0 mg of fenofibrate powder each, then put it into a 100.0 ml beaker containing 100.0 ml of distilled water, then dissolve it using a shaking thermostatic water bath at 37°C ± 0.5°C, stirring speed of 100 rpm for 7 days. Every 24 hours the concentration of fenofibrate dissolved until it forms a saturated solution is determined. The solution was analyzed by UV-Vis spectrophotometry at a wavelength of 233.8 nm.

Determination and Verification of Optimum Formulas of Fenofibrate Nanocrystals, Determination of the optimum area of phenofibate nanocrystal preparations using Design Expert 12 software. In this study a numerical approach was used to determine the optimum formulation. The data entered as a response is particle size, zeta potential and solubility test.

Differential Scanning Calorimetry (DSC), DSC analysis was carried out by means of the instrument being calibrated before being used using standard medium, then the sample was carefully weighed, 5.0 mg was put into an aluminum container, heated and measured from a temperature of 30-250oC, a constant heating rate of 10oC/minute with a flow of 20% nitrogen gas. mL/min endothermic and exothermic processes will be recorded on the recorder (Bonthagarala, 2015).

X-Ray Diffraction (XRD), X-ray diffraction analysis of sample powders was carried out at room temperature using an X-ray diffractometer (X'Pert PRO, Netherland). The measurement conditions are as follows: voltage 40 kV, current 30 mA, measurement analysis in the range 2 theta 5-50° and scanning speed 0.050 per second. The sample is placed on the sample holder (glass) and flattened to prevent particle orientation during sample preparation (Zaini, 2011). Analysis was performed on pure fenofibrate and fenofibrate nanocrystals.

Fourier Transform Infrared (FTIR), Tests were carried out on fenofibrate and fenofibrate nanocrystals. About 1.00-2.00 mg of sample powder is compressed onto a disc. The absorption spectrum was recorded at wave numbers 400-4000 cm-1 (Atia et.al 2020). This analysis will show a spectrum that describes the functional groups of fenofibrate compounds and fenofibrate nanocrystals.

Scanning Electron Microscope (SEM), The aluminum sample holder was coated with metallic paint, then rinsed with ethanol and then coated with a thin layer of adhesive. The

powder sample is placed in an aluminum sample holder and then coated with a thin layer of precious metal or gold. The voltage is set at 10 kV with a current of 12 mA, observed at various magnifications (Zaini, 2011). This analysis will show the morphology of fenofibrate particle shapes and fenofibrate nanocrystals.
(*Lokasi penelitian, Populasi dan sampel,Nomor Ijin Etik, Metode pengumpulan data, Analisis data, dll*)

RESULT

Particle Size Analyzer (PSA) and Zeta Potential

Table 3. Particle Size Analyzer (PSA) and Zeta Potential Measurements

Run	Tween 80 (%)	Grinding Speed (rpm)	Grinding Time (jam)	Particle Size (nm)	Zeta Potential
1	0,6	300	2	4792	-22,6
2	0,2	500	2	777,8	-30
3	0,6	500	2	4591	-27,5
4	0,2	300	1	916,4	-28,3
5	0,2	500	2	777,7	-29,3
6	0,2	300	2	1025	-27,4
7	0,6	300	2	2291	-29,3
8	0,2	500	1	1215	-20,5
9	0,6	300	1	2714	-21
10	0,6	500	1	1967	-11,4
11	0,6	500	1	2606	-15,5
12	0,2	300	1	901.5	-23,9
13	0,6	500	2	9291	-19,2
14	0,6	300	1	1409	-21,9
15	0,2	300	2	1882	-23,3
16	0,2	500	1	1444	-20,1

Particle size is very important in nanoparticle systems. The particle size of fenofibrate was measured using a PSA (Particle size Analyzer). The use of surfactant stabilizers affects the particle size and stability of the resulting nanocrystals. The surfactant stabilizer functions to stabilize suspensions by providing a charge on the surface of the nanoparticles so that there is repulsion between the particles so that agglomeration does not occur into larger particles (Toziopoulou et al., 2017).

Nanoparticles with Zeta Potential values greater than +30 mV or less than -30 mV usually have a high degree of stability. Dispersions with low zeta potential values will produce aggregates due to Van Der Waals attractions between particles (Murdock et al., 2008).

Solubiliton

Table 4. Solubility Nanocrystal Fenofibrate

Formula	Tween 80 (%)	Grinding Speed (rpm)	Grinding Time (Hours)	Solubility (µg/mL)
1	0,6	300	2	18,22
2	0,2	500	2	17
3	0,6	500	2	12,33
4	0,2	300	1	8,273
5	0,2	500	2	8,922
6	0,2	300	2	16
7	0,6	300	2	15,2
8	0,2	500	1	6,252
9	0,6	300	1	25
10	0,6	500	1	8,614
11	0,6	500	1	7,856
12	0,2	300	1	7,27
13	0,6	500	2	14,004
14	0,6	300	1	27,312
15	0,2	300	2	7,2
16	0,2	500	1	6,535

To evaluate the contribution of each of the three components and the quantitative effect of the different proportions and formulation variables on the solubility response (Y), surface response models were calculated with Design Expert software. The final equation of the model describing the solubility of fenofibrate nanocrystals can be written as follows:

Y = +8,069 +97,54 (A) -0,038 (B) -8,20 (C) -0,134 (A)(B) -18,64 (A)(C)+0,043 (B)(C)

Information:
Y = Solubility
A = Tween 80
B = Grinding Speed
C = Grinding Time

Based on the results of the equation, it shows that each component has an effect on the particle size of the fenofibrate nanosuspension. The tween 80 component has the greatest positive effect (+97.54) compared to speed (-0.037) and grinding time (-8.19). This study shows that the function of tween 80 as a surfactant greatly affects the solubility of fenofibrate nanocrystals, this is due to the properties of tween 80 which can reduce the surface tension between the active ingredient and the solvent used (X. Hu et al., 2017). The interaction of grinding speed and duration had the greatest positive effect (+0.043) compared to the interaction of tween 80 and speed (-0.134) and the interaction of tween 80 and grinding time (-18.64).

Determination and Verification of Optimum Formulas of Fenofibrate Nanocrystals

The data entered as a response is particle size, zeta potential and solubility test. The results of determining the optimum formula using weights and goals from the nanocrystal characterization test as listed in table 5.

Table 5. Values and weights of the characterization test for the optimum formula of fenofibrate nanocrystals

Lower limit	Upper limit	Goal	Characterization
200	999	In range	Particle Size
-30	+30	In range	Zeta Potential
0	15	In range	Solubility

Characteristics Test of Fenofibrate Nanocrystals

Differential Scanning Calorimetry (DSC), the sample (pure fenofibrate, poloxamer 188, mannitol, optimum formula) was carefully weighed 5.0 mg into an aluminum container, heated and measured from 30-250 oC. constant heating rate of 10 oC/minute with nitrogen gas flow of 20 mL/minute of endothermic and exothermic processes will be recorded in Figure 1 below.

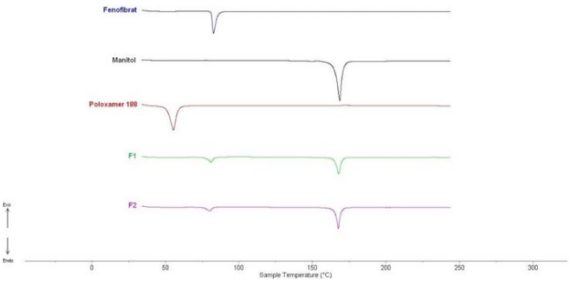

Figure 1. Differential Scanning Calorymetry (DSC)

X-Ray Diffraction, measurement conditions as follows: voltage 40 kV, current 30 mA, measurement analysis in the range 2θ 5-50° and scanning speed 0.05º per second. The sample is placed in the sample holder (glass) and leveled to prevent particle orientation during sample preparation. The results of X-ray diffraction can be concluded that there is a slight change in crystallity between pure fenofibrate and fenofibrate nanocrystals, as can be seen in Figure 2 below.

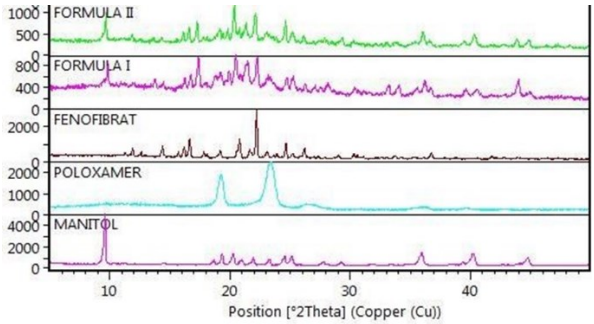

Figure 2. X-Ray Difractory

Fourier Transform Infra Red (FTIR), tests were carried out on fenofibrate, fenofibrate nanocrystals, poloxamer 188 and mannitol. About 1.0–2.0 mg of sample powder is compressed onto a disc. The absorption spectrum was recorded at wave numbers 400-4000 cm^{-1}. Fourier Transform Infra Red (FTIR), showed in figure 3 below.

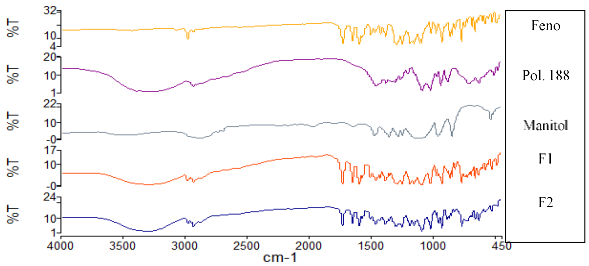

Figure 3. Fourier Transform Infra Red

Scanning Electron Microscope (SEM), SEM morphology testing by means of a sample is given a thin layer of gold-palladium Au (80%) and Pd (20%) using a current at 12 mA, a voltage of 20 kV. In SEM analysis, there are differences in the form of fenofibrate crystals and fenofibrate nanocrystals. In fenofibrate crystals, the average shape is irregularly shaped at 1000x magnification, and in fenofibrate nanocrystals it looks like lumps after 5000x magnification. The results can be seen in figure 4

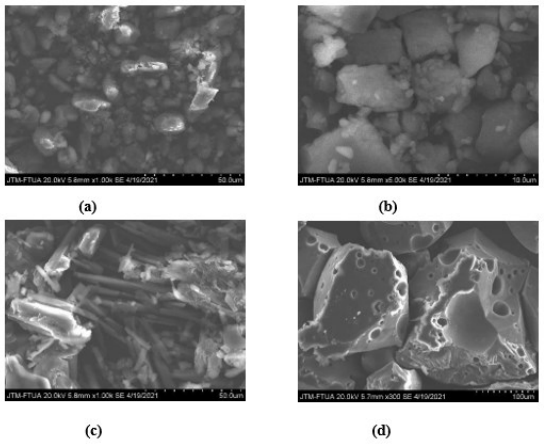

Figure 4. Scanning Electron Microscope (SEM) results, (a) fenofibrate, (b) fenofibrate nanocrystals, (c) mannitol, (d) poloxamer 188

DISCUSSION

Particle Size Analyzer (PSA) ANOVA analysis

To evaluate the contribution of each of the three components and the quantitative effect of different proportions and formulation variables on the particle size (Y) response, surface response models were calculated with Design Expert software. The final equation of the model describing the particle size of the fenofibrate nanosuspension can be written as follows:

Y = +7443.212 -14739.44 (A) -13.28 (B) -3617.23 (C) +24.25 (A)(B) +7677.13 (A)(C) +5, 20 (B)(C)

Information :
Y = Particle Size
A = Tweens 80
B = Speed
C = Grinding time

Based on the results of the equation, it shows that each component has an effect on the particle size of the fenofibrate nanosuspension. The tween 80 component, speed, and grinding time have a negative effect, where tween 80 has the greatest negative effect (-14739.44) compared to grinding time (-3617.23) and speed (-13.28), this shows that the tween 80, speed, and grinding time, had a negative effect which was predicted to increase the particle size. However, the interaction of the combination of tween 80 and other factors such as tween 80 and grinding time has the most positive effect (+7677.12) compared to the interaction of tween 80 and speed (+24.25) and the interaction of speed and grinding time (+5.20). . This proves that the combination of tween 80 with grinding speed and grinding time has a positive effect on particle size and grinding speed and grinding time also has a positive effect on particle size which is likely to reduce the particle size of the fenofibrate nanosuspension. In harmony, in this case, tween 80 acts as a surfactant which has properties as a surfactant in nanocrystal preparations, not as a form of nanocrystal preparations (X. Hu et al., 2017). The surfactants and polymers used have a role as stabilizers so that they can prevent particle aggregation from becoming larger at the nanocrystal size and increase solubility (AlYousef et al., 2018).

Zeta Potential ANOVA Analysis

To evaluate the contribution of each of the three components and the quantitative effect of the different proportions and variable formulations on the potential zeta response (Y), response surface models were calculated with Design Expert software. The final equation of the model describing the zeta potential of the fenofibrate nanosuspension can be written as follows:

Y = -43.425 -1.13 (A) +0.05 (B) +12.65 (C) +0.057 (A)(B) -7.25 (A)(C) -0.039 (B)(C)

Information :

Y = Zeta Potential
A = Tweens 80
B = Speed
C = Grinding time

Based on the results of the equation, it shows that each component has an effect on the zeta potential of the fenofibrate nanosuspension. The grinding time component has the greatest positive effect (+12.65) compared to speed (+0.050) and tween 80 (-1.13). This study shows that grinding time has a positive effect on zeta potential. The interaction of tween 80 and speed has the greatest positive effect (+0.057) compared to the interaction of tween 80 and grinding time (-7.25) and the interaction of speed and grinding time (-0.039). This proves that the grinding time has an effect on the zeta potential and interactions with tween 80 and the grinding speed also has an effect on the zeta potential of fenofibrate nanocrystals. Aligned with the grinding speed and grinding duration can affect the particle size and zeta potential (Toziopoulou et al., 2017).

Characterization of the optimum formula of fenofibrate nanocrystals

The desirability contour plot (figure 5) diagram shows that the formula selected as the optimum formula using Design Expert 12 software is a formula containing tween 80 0.200%, milling speed 500.00 rpm, milling time 1 hour. The desirability value is the value of the optimization objective function which shows the program's ability to fulfill the desired based on the set criteria. The range of desirability values is from 0 to 1.0. The desirability value that is closer to 1.0 indicates more perfect. The purpose of optimization is not to obtain a desirability value of 1.0, but to find the best conditions that bring together all objective functions (Raissi & Farzani, 2009).

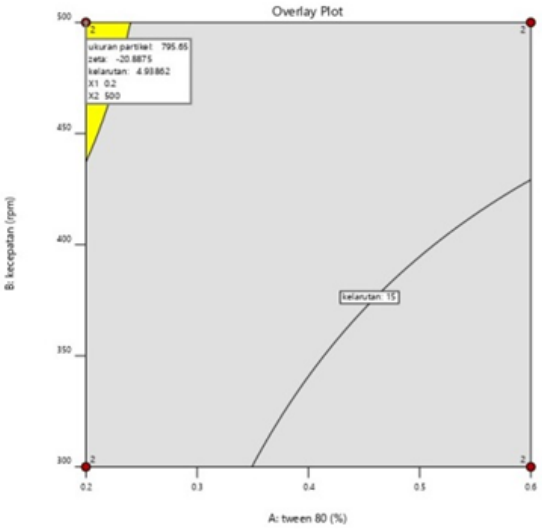

Figure 5. Contour plot diagram for optimum desirability formula

The optimum formula chosen in this study is one that has a desirability value close to 1. Desirability indicates the magnitude of the value in accordance with what is desired, achieving the maximum value on desirability indicates that the selection of goals in the three characterization tests is correct.

Differential Scanning Calorymetry (DSC), the maximum melting point of pure fenofibrate is 82.73ºC. The maximum melting point of mannitol is 168.591ºC. Maximum melting point of poloxamer 188 55.477ºC. The maximum melting point of the optimum formula for testing 1 is 80.997ºC and 167.74ºC. The maximum melting point for the optimum formula for testing 2 is 80.161ºC and 167.56ºC. The results of the DSC test showed that the melting point of fenofibrate appeared at a melting point of 82.73ºC. This result was different from the fenofibrate nanocrystals which appeared at a melting point of 168.591ºC which was similar to the melting point of mannitol and there was a decrease in the endothermic peak. This shows that pure fenofibrate which is made into fenofibrate nanocrystals with mannitol cryoprotectant material is not released in the system.

X-ray diffraction, in pure fenofibrate X-ray diffraction analysis, a series of intensity peaks were obtained at values of 2θ 11.86°, 14.38°, 16.61°, 20.79°, 22.15°, 24.62°, 26, 17°, and 36.72°. The poloxamer 188 diffraction pattern shows intensity peaks at 2θ values, namely 19.41° and 23.7°. The mannitol diffraction

pattern showed intensity peaks at 2θ values, namely 9.6°, 16.5°, 18.0°, 25.78°. The results of the X-ray diffraction test show that the peak intensity value of 2θ fenofibrate appears at 11.86°, 14.38°, 16.61°, 20.79°, 22.15°, 24.62°, 26.17°, and 36.72° this result is different from the fenofibrate nanocrystals which appear at peak intensity values of 2θ9.6°, 16.5°, 18.0°, 25.78° which are similar to the melting point of mannitol and there are differences in crystallity characteristics where the crystallinity of the nanocrystals fenofibrate is denser which shows it is amorphous. This shows that pure fenofibrate which is made into fenofibrate nanocrystals with mannitol cryoprotectant material is not released in the system.

FTIR analysis, pure fenofibrate shows an absorption of 1729.24 cm^{-1} for the C=O ester group, 1651.12 cm^{-1} for the C=O ketone group, 1302.96 cm^{-1} for the ether group and 2983.01 cm^{-1} for aromatic strain. The spectrum of poloxamer 188 shows absorption bands due to OH (3600–3400 cm^{-1}) and C-O (1112 cm^{-1}) strains. Mannitol shows C–H or O–H strain bands in the region between 2800 cm^{-1} and 3700 cm^{-1} and C–O between 900 cm^{-1} and 1500 cm^{-1}. The nanocrystals showed a strain of 1732.13 cm^{-1} C=O for the ester group, 1650.16 cm^{-1} for the ketone group C=O and 2968.72 cm^{-1} for the aromatics. The results of the FTIR test show that fenofibrate and fenofibrate nanocrystals do not appear to differ in functional groups. This shows that pure fenofibrate made into fenofibrate nanocrystals with mannitol cryoprotectant does not change the functional groups in the system.

CONCLUSION

The optimum formula with tween 80 components, grinding speed and grinding time in the manufacture of fenofibrate nanocrystals using the Factorial Design method obtained 0.2% tween 80, grinding speed of 500 rpm and grinding time of 1 hour. The critical parameter test results for the optimum formula obtained a particle size of 775.966 nm, a zeta potential of -21.302 mV and a solubility of 5.977 µg/mL. The DSC test showed that there was a difference in the melting point peaks and a decrease in crystal intensity between pure fenofibrate and fenofibrate nanocrystals. The FTIR test showed no difference in functional groups between pure fenofibrate and fenofibrate nanocrystals. The XRD test showed that there was a difference in peak crystal intensity between pure fenofibrate and fenofibrate nanocrystals. The SEM analysis shows that there are differences in shape and magnification used between pure fenofibrate and fenofibrate nanocrystals.

REFERENCES

1. [Anonim]. 2014. Farmakope Indonesia. Edisi V. Jakarta: Departemen Kesehatan Republik Indonesia.
2. Abdelwahed, W., Degobert, G., Stainmesse, S., & Fessi, H. (2006). Freeze-drying of nanoparticles : Formulation , process and storage considerations ☆. 58, 1688–1713.
3. Afif, H.F. (2008). Studi Pra-feasibilitas dengan sirkuit benefiasi logam tanah jarang berbasis pasir monazite. Depok: Fakultas Teknik Universitas Indonesia.
4. AlYousef, Z. A., Almobarky, M. A., & Schechter, D. S. (2018). The effect of nanoparticle aggregation on surfactant foam stability. Journal of Colloid and Interface Science, 511, 365–373.
5. Bastami, Z., Taheri, A., & Soltanpour, S. (2015). Formulation, optimization and characterization of gemfibrozil nanocrystals prepared by wet milling technique. Asian Journal of Pharmaceutics, 9(1), 19–22.
6. Bonthagarala, B. (2015). A review on significance of nanocrystals in drug delivery. August 2013.
7. Bouchemal, K., Briançon, S., Perrier, E., & Fessi, H. (2004). Nano-emulsion formulation using spontaneous emulsification : solvent , oil and surfactant optimisation. 280, 241–251.
8. Buraphacheep, V., & Morakul, B. (2015). ScienceDirect Nanocrystals for enhancement of oral bioavailability

of poorly water-soluble drugs. Asian Journal of Pharmaceutical Sciences, 10(1), 13–23.
9. Chan, H., Chi, P., & Kwok, L. (2011). Production methods for nanodrug particles using the bottom-up approach ☆. Advanced Drug Delivery Reviews, 63(6), 406–416.
10. Choi, J. Y., Yoo, J. Y., Kwak, H. S., Nam, B. U., & Lee, J. (2005). Role of polymeric stabilizers for drug nanocrystal dispersions. Current Applied Physics, 5(5), 472–474.
11. Chowdary, K. P. R., & Enturi, V. (2011). Enhancement of dissolution rate and formulation development of efavirenz tablets employing starch citrate-a new modified starch. Journal of Applied Pharmaceutical Science, 1(5), 119–123.
12. Colombo, M., Orthmann, S., Bellini, M., Staufenbiel, S., & Bodmeier, R. (2017). Influence of Drug Brittleness, Nanomilling Time, and Freeze-Drying on the Crystallinity of Poorly Water-Soluble Drugs and Its Implications for Solubility Enhancement. AAPS PharmSciTech, 18(7), 2437–2445.
13. Dibaei, M., Rouini, M. R., Sheikholeslami, B., Gholami, M., & Dinarvand, R. (2019). The effect of surface treatment on the brain delivery of curcumin nanosuspension: In vitro and in vivo studies. International Journal of Nanomedicine, 14, 5477–5490.
14. Eerdenbrugh, Bernard Van, Mooter, G. Van Den, & Augustijns, P. (2008). Top- down production of drug nanocrystals : Nanosuspension stabilization , miniaturization and transformation into solid products. 364, 64–75.
15. Fernandes, A. R., Ferreira, N. R., Fangueiro, J. F., Santos, A. C., Veiga, F. J., Cabral, C., Silva, A. M., & Souto, E. B. (2017). Ibuprofen nanocrystals developed by 22 factorial design experiment: A new approach for poorly water-soluble drugs. Saudi Pharmaceutical Journal, 25(8), 1117–1124.
16. Ghosh, I., Schenck, D., Bose, S., & Ruegger, C. (2012). Optimization of formulation and process parameters for the production of nanosuspension by wet media milling technique: Effect of Vitamin e TPGS and nanocrystal particle size on oral absorption. European Journal of Pharmaceutical Sciences, 47(4), 718–728.
17. Hu, J., Dong, Y., Ng, W. K., & Pastorin, G. (2018). Preparation of drug nanocrystals embedded in mannitol microcrystals via liquid antisolvent precipitation followed by immediate (on-line) spray drying. Advanced Powder Technology, 29(4), 957–963.
18. Hu, X., Yang, F. F., Wei, X. L., Yao, G. Y., Liu, C. Y., Zheng, Y., & Liao, Y. H.
19. (2017). Curcumin acetate nanocrystals for sustained pulmonary delivery: Preparation, characterization and in vivo evaluation. Journal of Biomedical Nanotechnology, 13(1), 99–109.
20. Ige, P. P., Baria, R. K., & Gattani, S. G. (2013). Fabrication of fenofibrate nanocrystals by probe sonication method for enhancement of dissolution rate and oral bioavailability. Colloids and Surfaces B: Biointerfaces, 108, 366– 373.
21. Jeon, S., Thajudeen, T., & Hogan, C. J. (2015). Evaluation of nanoparticle aggregate morphology during wet milling. Powder Technology, 272, 75–84.
22. Jermain, S. V., Brough, C., & Williams, R. O. (2018). Amorphous solid dispersions and nanocrystal technologies for poorly water-soluble drug delivery – An update. International Journal of Pharmaceutics, 535(1–2), 379–392.
23. Jones, A., Rigopoulos, S., & Zauner, R. (2005). Crystallization and precipitation engineering. 29(April), 1159–1166.

24. Junghanns, J. A. H. (2008). Nanocrystal technology , drug delivery and clinical applications. 3(3), 295–309.
25. Karagianni, A., & Peltonen, L. (2020). Production of itraconazole nanocrystal- based polymeric film formulations for immediate drug release. Pharmaceutics, 12(10), 1–10.
26. Kevadiya, B. D., Barvaliya, M., Zhang, L., Anovadiya, A., Brahmbhatt, H., Paul, P., & Tripathi, C. (2018). Fenofibrate nanocrystals embedded in oral strip- films for bioavailability enhancement. Bioengineering, 5(1), 1–17.
27. Kumar, R., & Siril, P. F. (2018). Enhancing the Solubility of Fenofibrate by Nanocrystal Formation and Encapsulation. AAPS PharmSciTech, 19(1), 284– 292.
28. Lee, J., & Cheng, Y. (2006). Critical freezing rate in freeze drying nanocrystal dispersions. Journal of Controlled Release, 111(1–2), 185–192.
29. Leuner, C., & Dressman, J. (2000). Improving drug solubility for oral delivery using solid dispersions. European Journal of Pharmaceutics and Biopharmaceutics, 50(1), 47–60.
30. Liu, P., Rong, X., Laru, J., Veen, B. Van, Kiesvaara, J., Hirvonen, J., Laaksonen, T., & Peltonen, L. (2011). Nanosuspensions of poorly soluble drugs : Preparation and development by wet milling. International Journal of Pharmaceutics, 411(1–2), 215–222.
31. Ma, Y., Zheng, Y., Zeng, X., Jiang, L., Chen, H., Liu, R., Huang, L., & Mei, L. (2011). Novel docetaxel-loaded nanoparticles based on PCL-Tween 80 copolymer for cancer treatment. International Journal of Nanomedicine, 6, 2679–2688.
32. Madgulkar, A., Bhalekar, M., & Khabiya, P. N. (2019). Nanoparticulates of Fenofibrate for Solubility Enhancement : Ex-Vivo. 9(4), 155–163.
33. Merisko-Liversidge, E., Liversidge, G. G., & Cooper, E. R. (2003). Nanosizing: A formulation approach for poorly-water-soluble compounds. European Journal of Pharmaceutical Sciences, 18(2), 113–120.
34. Moorthi, C., & Kathiresan, K. (2013). Fabrication of highly stable sonication assisted curcumin nanocrystals by nanoprecipitation method. Drug Invention Today, 5(1), 66–69.
35. Murdock, R. C., Braydich-stolle, L., Schrand, A. M., Schlager, J. J., Hussain, S. M., & Al, M. E. T. (2008). Characterization of Nanomaterial Dispersion in Solution Prior to In Vitro Exposure Using Dynamic Light Scattering Technique. 101(2), 239–253.
36. Ochi, M., Kawachi, T., Toita, E., Hashimoto, I., Yuminoki, K., Onoue, S., & Hashimoto, N. (2014). Development of nanocrystal formulation of meloxicam with improved dissolution and pharmacokinetic behaviors. International Journal of Pharmaceutics, 474(1–2), 151–156.
37. Pande, V. V., & Abhale, V. N. (2016). Nanocrystal technology: A particle engineering formulation strategy for the poorly water soluble drugs. Der Pharmacia Lettre, 8(5), 384–392.
38. Pawley, J. (1997). The Development of Field-Emission Scanning Electron Microscopy for Imaging Biological Surfaces. 19, 324–336.
39. Peltonen, L., & Hirvonen, J. (2010). Pharmaceutical nanocrystals by nanomilling: Critical process parameters, particle fracturing and stabilization methods. Journal of Pharmacy and Pharmacology, 62(11), 1569–1579.
40. Perecin, C., Cerize, N., Chitta, V., Gratens, X., Léo, P., de Oliveira, A., & Yoshioka, S. (2016). Magnetite Nanoparticles Encapsulated with PCL and Poloxamer by Nano Spray Drying Technique. Nanoscience and Nanotechnology, 6(4), 68–73.

41. Rachmawati, H., Yanda, Y. L., Rahma, A., & Mase, N. (2016). Curcumin-loaded PLA nanoparticles: Formulation and physical evaluation. Scientia Pharmaceutica, 84(1), 191–202.
42. Rao, Y., Kumar, M., & Apte, S. (2008). Formulation of Nanosuspensions of Albendazole for Oral Administration. Current Nanoscience, 4(1), 53–58.
43. Rawle, A. F. (n.d.). Analytical Tools for Suspension Characterization.
44. Retnowati, D., & Setyawan, D. (2010). Peningkatan Disolusi Ibuprofen dengan Sistem Dispersi Padat Ibuprofen-PVP K90. Majalah Farmasi Airlangga, 8(April), 24–28.
45. Shan, N., & Zaworotko, M. J. (2008). The role of cocrystals in pharmaceutical science. 13(May).
46. Sooväli, L., Rõõm, E. I., Kütt, A., Kaljurand, I., & Leito, I. (2006). Uncertainty sources in UV-Vis spectrophotometric measurement. Accreditation and Quality Assurance, 11(5), 246–255.
47. Tantri, G. K. D., Widiharih, T., & Wuryandari, T. (2015). Analisis desain faktorial fraksional 2. Jurnal Gaussian, 4(3), 497–505.
48. Terzopoulou, Z., Klonos, P. A., Kyritsis, A., Tziolas, A., Avgeropoulos, A., Papageorgiou, G. Z., & Bikiaris, D. N. (2019). Interfacial interactions, crystallization and molecular mobility in nanocomposites of Poly(lactic acid) filled with new hybrid inclusions based on graphene oxide and silica nanoparticles. Polymer, 166(January), 1–12.
49. Toziopoulou, F., Malamatari, M., Nikolakakis, I., & Kachrimanis, K. (2017). Production of aprepitant nanocrystals by wet media milling and subsequent solidification. International Journal of Pharmaceutics, 533(2), 324–334.
50. Tuomela, A., Hirvonen, J., & Peltonen, L. (2016). Stabilizing agents for drug nanocrystals: Effect on bioavailability. Pharmaceutics, 8(2).
51. Van Eerdenbrugh, B., Froyen, L., Martens, J. A., Blaton, N., Augustijns, P., Brewster, M., & Van den Mooter, G. (2007). Characterization of physico- chemical properties and pharmaceutical performance of sucrose co-freeze- dried solid nanoparticulate powders of the anti-HIV agent loviride prepared by media milling. International Journal of Pharmaceutics, 338(1–2), 198– 206.
52. Wisudyaningsih, B. (2012). Studi preformulasi: validasi metode spektrofotometri ofloksasin dalam larutan dapar fosfat. Stomatognatic, 9(2), 77–81.
53. Yan, F., Zhang, C., Zheng, Y., Mei, L., Tang, L., Song, C., Sun, H., & Huang, L. (2010). The effect of poloxamer 188 on nanoparticle morphology, size, cancer cell uptake, and cytotoxicity. Nanomedicine: Nanotechnology, Biology, and Medicine, 6(1), 170–178.
54. Ye, X., Patil, H., Feng, X., Tiwari, R. V., Lu, J., Gryczke, A., Kolter, K., Langley,
55. N., Majumdar, S., Neupane, D., Mishra, S. R., & Repka, M. A. (2016). Conjugation of Hot-Melt Extrusion with High-Pressure Homogenization: a Novel Method of Continuously Preparing Nanocrystal Solid Dispersions. AAPS PharmSciTech, 17(1), 78–88.
56. Zaini, E. (2011). TRIMETOPRIM MELALUI METODE KO-KRISTALISASI.
57. Zielińska, A., Ferreira, N. R., Feliczak-Guzik, A., Nowak, I., & Souto, E. B. (2020). Loading, release profile and accelerated stability assessment of monoterpenes-loaded solid lipid nanoparticles (SLN). Pharmaceutical Development and Technology, 25(7), 832–844.